JPPIPA 9(8) (2023)

Jurnal Penelitian Pendidikan IPA

Journal of Research in Science Education

http://jppipa.unram.ac.id/index.php/jppipa/index

Identification of Liquefaction-Potential Zones Using the Gravity Method in Lolu Village, Central Sulawesi

Meschac T Silalahi[1*], Darharta Dahrin[1], Dadi Abdurrahman[1], Adrin Tohari[2]

[1] Department of Geophysics Engineering, Faculty of Mining and Petroleum Engineering, Institute of Technology Bandung, Bandung, Indonesia.

[2] Research Center for Geotechnology, National Research and Innovation Agency (BRIN), Bandung, Indonesia.

Received: June 4, 2023
Revised: July 30, 2023
Accepted: August 25, 2023
Published: August 31, 2023

Corresponding Author:
Meschac T Silalahi
meschacts@gmail.com

DOI: 10.29303/jppipa.v9i8.4830

Abstract: A seismic event of magnitude 7.5 struck the Palu region in Central Sulawesi on September 28, 2018, precipitating a subsequent calamity in the form of a tsunami measuring 4-7 meters in height. This catastrophe was further compounded by the occurrence of liquefaction, leading to extensive devastation and a significant loss of life. In order to identify areas susceptible to liquefaction, it is anticipated that the employment of the gravity method, renowned for its capacity to discern density fluctuations associated with the mass of voluminous materials over a considerable detection range, will prove instrumental. The investigation of parameters and the characterization of liquefaction phenomena in regions previously afflicted by liquefaction disasters can be instrumental in devising strategies for mapping zones that are predisposed to such occurrences. The present study seeks to employ geophysical methods, specifically the gravity method, to delineate zones with the potential for liquefaction within the Lolu Village at Palu City, Central Sulawesi. Through the application of techniques designed to isolate regional and residual anomalies, it is envisaged that a clearer understanding of anomalies situated in shallower regions can be attained, with a specific focus on residential areas. Notably, due to liquefaction, approximately half of the residential areas have shifted a considerable distance of around 132 meters from their original positions. To facilitate the interpretation of subsurface layers, two-dimensional cross-sections are modeled to intersect the displaced and stationary areas. The residual map reveals discernible variations in anomaly values, with lower values observed in the areas that experienced liquefaction-induced movement. Subsurface modeling further demonstrates the presence of three distinct rock layers, namely a sandy layer, a gravel layer, and a rock layer. Additionally, the modeling depicts the formation of canals composed of hard rock, exhibiting varying thicknesses within the surface layer as a consequence of the liquefaction event in 2018. The existence of these canals serves as an indicator that when the sandy layer becomes saturated with water, it will flow along the topographical gradient, following the path of the subterranean canals that have formed.

Keywords: Gravity; Liquefaction; Lolu village; 2D modelling

Introduction

A seismic disaster of magnitude 7.5 Mw occurred in the Palu region of Central Sulawesi on September 28, 2018. Subsequently, this earthquake led to a secondary disaster, namely a tsunami with a height of 4-7 meters (Beaudouin et al., 2003; Socquet et al., 2006; Bellier et al., 2006; Watkinson & Hall, 2017), which was further accompanied by the phenomenon of liquefaction. This phenomenon resulted in significant infrastructure damage, including a substantial loss of life. One of the active faults in Sulawesi is the Palu-Koro fault, which extends approximately 220 km from Palu City (north) to Malili (south), reaching the Bone Gulf. This fault exhibits sinistral movement at a rate of 27-43 mm/year (Helmers, et al., 1990; Bellier et al., 2001). The tectonic earthquake triggered the occurrence of liquefaction, attributed to the seismic vibrations altering the soil pore conditions,

How to Cite:
Silalahi, M. T., Dahrin, D., Abdurrahman, D., & Tohari, A. (2023). Identification of Liquefaction-Potential Zones Using the Gravity Method in Lolu Village, Central Sulawesi. *Jurnal Penelitian Pendidikan IPA*, *9*(8), 6206–6212. https://doi.org/10.29303/jppipa.v9i8.4830

causing water infiltration and subsequently weakening the solid material's cohesive bonds. Consequently, the soil's properties transitioned from solid to liquid, significantly impacting structures situated on liquefied ground (Sawicki & Mierczyński, 2009; Chen et al., 2021).

Kramer (1996) elaborated on the mechanism of liquefaction, concluding that it involves the loss of shear strength in saturated, cohesionless soils due to increased pore water pressure and decreased effective stress during cyclic loading. Generally, liquefaction occurs in earthquake-prone areas with shallow groundwater tables and poorly consolidated soils. Understanding subsurface conditions within a specific area aids in mapping or zoning potentially liquefaction-prone regions. Geophysical methods offer the capability to assist in subsurface condition identification. The gravity method is one of several geophysical techniques; Hinze (1990) underscored its reliability in interpreting subsurface conditions, particularly pertaining to geological structures.

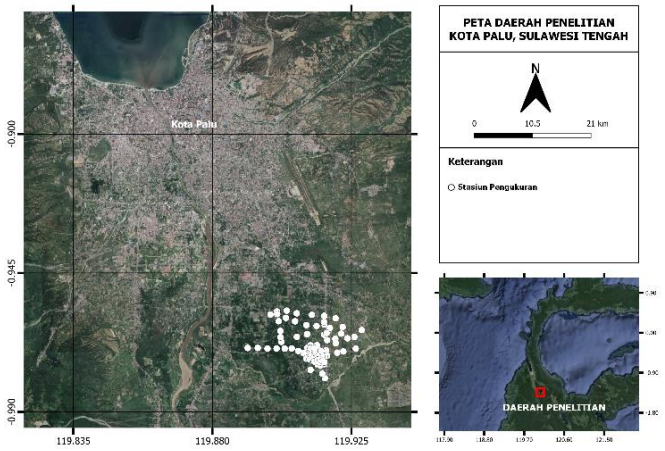

Figure 1. Gravity research area

Studying the parameters and identifying the characteristics of liquefaction phenomena in regions that have experienced liquefaction disasters can be employed for developmental purposes, particularly in mapping potential zones susceptible to liquefaction. In this context, geophysical methods, specifically the gravity method, will be utilized to map potential liquefaction-prone zones in the study area of Lolu Village, Palu City, Indonesia.

Geology Regional

In terms of stratigraphy, the Palu region is composed of rocks ranging from the Cretaceous to the Quaternary period (Charles et al., 1988). The basement component and the oldest rocks constitute the Palu Metamorphic Complex (PMC). Leeuwen (2016) stated through research that the lithology comprising the PMC consists of regionally metamorphosed rocks ranging from greenschist to amphibolite facies, as well as lower contact metamorphic rocks and high-pressure/ultrahigh-pressure metamorphic rocks (HP/UHP). According to Soekamto et al. (1973) and Sukarna et al. (1993), the lithology within the Palu Basin consists of alluvium and coastal deposits (Qa), which are the youngest constituents found at the surface, along with the Celebes Molasse Sarasin and Sarasin rocks, also referred to as the Pakuli Formation (Qp), Lariang Formation, Latimojong Formation, Gumbasa and Wana Complexes, Tinombo Ahlburg Formation, Metamorphic Batuam Complex, as well as Granite and Granodiorite.

Bradley et al. (2019), Bao et al. (2019), Hazarika (2021), Kiyota et al. (2020), and Andika (2023) have conducted research on liquefaction occurrences in Lolu Village. Several conclusions have been drawn, indicating that liquefaction in Lolu Village is a consequence of shallow water being used for irrigation of fields and plantations by residents. Additionally, the presence of confined aquifers has also triggered surface liquefaction events (Okamura et al., 2020; Kusumawardani et al., 2021). Seismic tomography has revealed the presence of grabens in areas affected by liquefaction (Watkinson & Hall, 2019).

Method

The research is situated in Lolu Village, Palu City, Central Sulawesi. The utilized data is the outcome of gravity acquisition performed at the research location, covering an area of approximately 14.8 km2, with a total of 123 measurement points. The gravity data collection took place in October 2022. The processing of the acquired gravity data will commence with the application of commonly utilized corrections, including tidal correction, drift correction, and latitude correction. Subsequently, corrections for free-air (FAC), Bouguer (BC), and terrain (TC) effects will be implemented, resulting in the generation of the complete Bouguer anomaly (CBA).

Gravity Anomaly

Gravity anomaly refers to the disparity between the observed gravity that has been adjusted to the geoid surface and the theoretical gravity. To convert the observed gravity to the geoid surface, several reductions are necessary, including Bouguer reduction, free-air reduction, and field reduction. During gravity measurements at a specific point, three values are computed: the standard gravity value, the measured gravity value, and the reduced gravity value. These three gravity values typically do not yield identical results due to the influence of subsurface mass anomalies beneath the measurement point on the

observed gravity value. The disparity between the standard gravity value and the measured gravity value is termed the gravity anomaly. Gravity anomalies can be categorized into different types:

$$\begin{aligned} \Delta g &= g\ obs - \gamma = gravity\ anomaly \\ \Delta g_0 &= g_0 - g = free\ air\ anomaly \\ \Delta g_0' &= \Delta g_0' - g = Bouguer\ anomaly \end{aligned} \quad (1)$$

The free-air anomaly provides information about the actual gravity field along the Earth's surface. Its magnitude is formulated as follows:

$$\Delta g_{free\ air} = \left(g_{obs} + g_{free\ air}\right) - g_0 \quad (2)$$

The Bouguer anomaly portrays information about the subsurface mass beneath the Earth's surface, and its formulation is expressed as follows (Telford, 1990):

$$CBA = G_{obs} - G_\theta + FAC - BC + TC \quad (3)$$

Gravity Anomaly Separation

The Bouguer anomaly is the result of summing up the regional anomaly and the residual anomaly. The regional anomaly originates from greater depths, while the residual anomaly emanates from shallower depths. Both of these anomalies overlap within the Bouguer anomaly. To study geological conditions at shallower depths, the separation of regional and residual anomalies can be performed. One method to achieve this separation is by employing the Moving Average method. The Moving Average technique involves averaging anomaly values. The outcome of averaging these anomalies corresponds to the regional anomaly (Abdelrahman & El-Araby, 1996). Mathematically, the moving average is expressed by the following formula:

$$R(x_i, z, s) = \frac{A}{2}\left\{2((x_i^2 + z^2)^{-q} - \left(\left(x_i^2 - s\right)^2 + z^2\right)^{-q} - \left(\left(x_i^2 + s\right)^2 + z^2\right)^{-q}\right\} \quad (4)$$

2D Forward Modeling

In geophysics, modeling is an endeavor aimed at obtaining subsurface conditions at a location where data measurements are taken. The sought-after model is one that generates a response that closely matches or fits the observed data or field-acquired data (Grandis, 2009). To achieve alignment between theoretical and field-acquired data in forward modeling, a trial and error process is undertaken by adjusting the model's parameter values. Consequently, it can be inferred that forward modeling methods encompass not only the computation of model responses but also a manual trial and error process with the goal of obtaining a model that provides a response consistent with the data. This congruent response is considered to represent the actual geological conditions beneath the surface (Grandis, 2009). In this study, 2D forward gravity modeling is conducted using the software Model Vision version 13.0.

Results and Discussion

The focal point of this research lies within a residential complex in Lolu Village that directly experienced the effects of the liquefaction phenomenon. Figure 2 illustrates the residential complex situated in the liquefaction area, captured one month prior to the liquefaction event caused by an earthquake, precisely in August 2018.

Figure 2. Residential complex before earthquake

Figure 3 illustrates the condition of half of the residential complex that experienced displacement during the liquefaction event in October 2018 (displacements are marked by orange boxes and arrows). One of the houses, indicated by a blue circle, underwent a change in position towards the orange circle. The displacement distance covered approximately ±150 meters.

Figure 3. Residential complex after earthquake

Gravity Data Processing

Following the necessary corrections applied to the gravity data, a complete Bouguer anomaly map is obtained. Figure 4 displays the complete Bouguer anomaly, indicating that the eastern portion of the research area exhibits higher anomaly values compared to the western area, where the anomaly values tend to be lower. This variation can be attributed to the presence of thicker alluvial layers resulting from deeper underlying hard rock layers in the western part of the research area, while the reverse is true for the eastern area, where hard Rock layers are shallower.

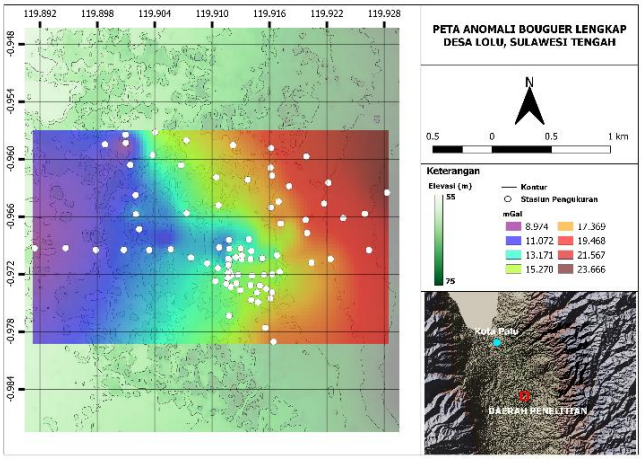

Figure 4. Complete bouguer anomaly

The separation of regional and residual anomalies was accomplished using the moving average method with an 11x11 window size. This separation process was conducted to distinguish between deeper and shallower anomalies within the research area. The residual anomaly map is essential for this study as it allows for the examination of density distribution in shallower regions. This is particularly pertinent given that liquefaction occurrences take place in shallower or near-surface areas.

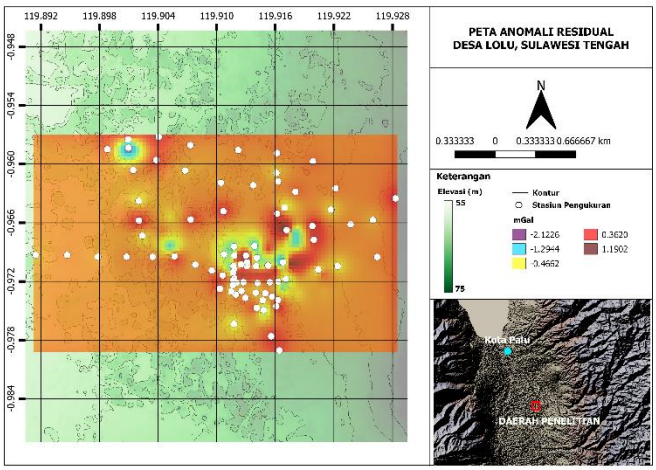

Figure 5. Residual anomaly

2D Modeling

Within the research area, there are zones that have experienced liquefaction and others that have not. A 2D modeling approach was employed to provide an insight into the subsurface geological conditions of the research area. Subsurface modeling was conducted using the residual anomaly data from the research area. The maximum modeling depth extended up to 150 meters from the ground surface.

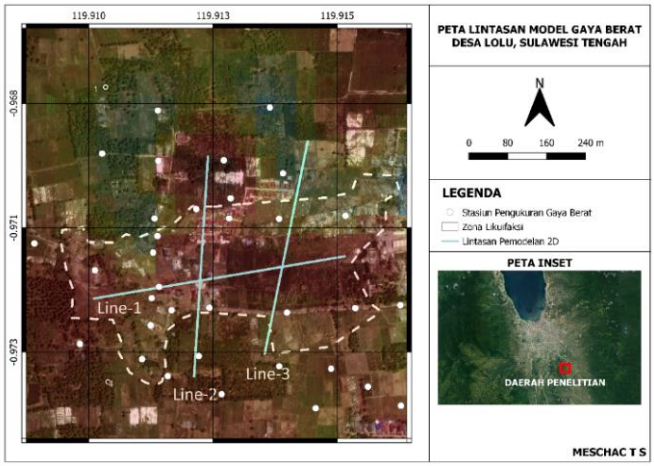

Figure 6. Cross-sectional profiles (Line-1, Line-2, and Line-3) were selected within the research area for subsurface modeling purposes. The liquefaction-prone area is delineated by dashed lines (Watkinson & Hall, 2019) on the profiles

From the forward modeling results, it is evident that there are three rock layers. It is assumed that the uppermost layer represents a sandstone layer, serving as the surface soil. This surface layer is saturated due to the influence of irrigation practices employed for local plantations (Bradley et al., 2019; Socquet et al., 2019; Jaya et al., 2019). Below this layer lies a coarser rock layer known as gravel or pebbles, and the basal layer is composed of hard rock. The density value assigned to the soil or surface layer is 1.5 g/cc^3.

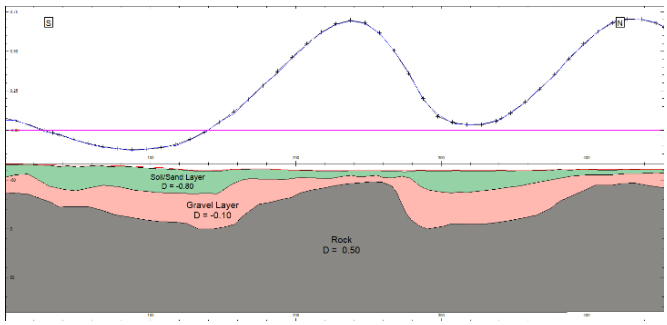

Figure 7. 2D gravity model of Line-1

The density value for the second layer is 2.2 g/cc^3, while the density value for the hard rock layer is 2.8 g/cc^3. The figure represents a cross-sectional profile for

the 2D subsurface modeling along Line-1. In the western area, there are undulations in both high and low anomaly values. These undulations indicate the presence of a subsidence in the basement or hard rock layer, forming some sort of channel or conduit. This channel or conduit influences the direction of mass movement on the surface. The assumed variation in surface layer thickness in the western area is attributed to mass displacement during liquefaction events.

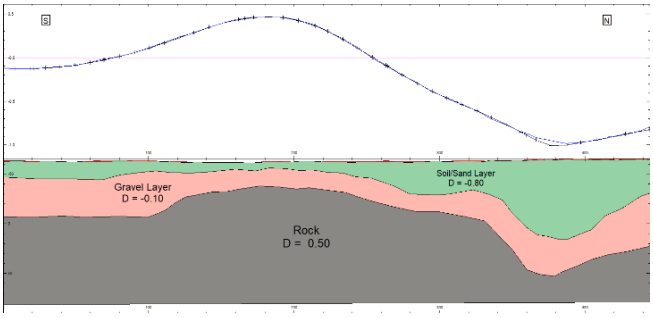

Figure 8. 2D gravity model of Line-2

The presence of an aquifer is a crucial factor in the occurrence of liquefaction (Cummins, 2019). According to Hazarika et al. (2021), aquifers are typically located at a depth of approximately ±25 meters from the ground surface. The second layer in the gravity modeling results is situated at a depth of around 10-60 meters beneath the surface. This layer is suspected to contain the aquifer.

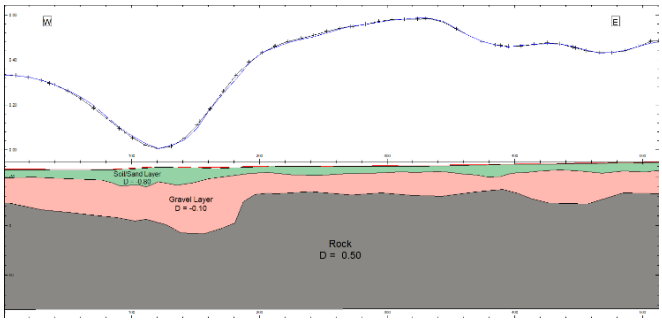

Figure 9. 2D gravity model of Line-3

The modeling along Line-2 traverses through both liquefied and stable areas. The stable area to the north is indicated by high anomalies, whereas the liquefied area is marked by low anomalies. The subsurface geological conditions influence the mass movement on the surface. The decrease in anomaly values in the area of mass movement is attributed to the formation of a channel due to the presence of a hard layer beneath the surface.

Line-3 intersects low anomalies to the north and progressively higher anomalies to the south. This anomaly variation is caused by the thickness of the alluvial layer in the northern section, which fills the basin of the basement layer. The stability in the north is assumed due to the elevated basement layer in the western part of the Line-3 path, effectively restraining mass movement from the surface layer. The liquefied area in the southern part is attributed to the topographic slope and saturated soil conditions on the surface. Previous research by Rahayu (2021) has investigated the cross-sections of Line-2 and Line-3 using borehole sampling methods. Through borehole data testing, it was found that areas with deeper basement depressions exhibit lower safety factor values compared to areas where the basement layer is at shallower depths. Based on grain size distribution curves presented by Tsuchida (1970), the northern sections of Line-2 and Line-3 are composed of materials with relatively high porosity and permeability, making them more vulnerable to liquefaction at shallow depths (0-19 meters).

Conclusion

From the gravity research in the liquefaction area of Lolu Village, it has been determined that the liquefaction-prone area comprises three relatively distinct rock layers based on their density contrast values. The first layer constitutes soil, with a density contrast value of -0.8 g/cc. The second layer consists of coarser-grained material, exhibiting a density contrast value of -0.1 g/cc. Meanwhile, the third layer, characterized as strong or stable, possesses a density contrast value of 0.5 g/cc. The surface layer is identified as highly susceptible to liquefaction based on borehole sampling studies.

Acknowledgments

I would like to express my heartfelt gratitude to all parties who have supported me in completing this research. Especially to my supervising lecturer, Dr. Darharta Dahrin, M.S and Dr. Dadi Abdurrahman, S.T, M.T, who have provided extensive assistance in terms of ideas, time and unwavering support troughout the entire duration of this research, both technically and non-technically. I am also thankful to Mr. Adrin Tohari, as the contributor of the data that was examined in this study. Finally yet importantly, I would like to extend my thanks to all my colleagues who have supported me in various ways.

Author Contributions

Conceptualization, Meschac T. Silalahi. and Dr. Darharta Dahrin, M.S; methodology, Meschac T. Silalahi, Dr. Darharta Dahrin, M.S., Dr. Dadi Abdurrahman, S.T, M.T., Adrin Tohari,; software, Meschac T. Silalahi and Dr. Dadi Abdurrahman, S.T, M.T.; validation, Dr. Darharta Dahrin, M.S and Dr.Dadi Abdurrahman, S.T., M.T.; writing—original draft preparation, Meschac T. Silalahi.

Funding

This research received no external funding.

Conflicts of Interest

The authors declare no conflict of interest.

References

Abdelrahman, E. M., & El-Araby, T. M. (1996). Shape and Depth Solutions from Moving Average Residual Gravity Anomalies. *Journal of Applied Geophysics, 36*(2-3), 89-95. https://doi.org/10.1016/S0926-9851(96)00038-9

Andika, P. P., Tohari, A., Yudistira, T., Soebowo, E., & Arifin, J. (2023): Understanding of Flow Liquefaction in Lolu Village Based on Seismic Refraction Tomography Method. 3rd *International Conference on Disaster Management*. IOP Conference Series: Earth and Environmental Science vol. 1173 (2023) 012029. https://doi.org/10.1088/1755-1315/1173/1/012029

Bao, H., Ampuero, J. P., Meng, L., Fielding, E. J., Liang, C., Milliner, S. W. D., Feng, T., & Huang, H. (2019). Early and Persistent Supershear Rupture of the 2018 Magnitude 7.5 Palu Earthquake. *Nat Geosci, 12*, 200–205. https://doi.org/10.1038/s41561-018-0297-z

Beaudouin, T., Bellier, O., & Sebrier, M. (2003). Present-Day Stress and Deformation Fields within the Sulawesi Island Area (Indonesia): Geodynamic Implications. *Bulletin de la Societe Geologique de France, 174*(3), 305-317. Retrieved from https://www.researchgate.net/publication/281538707

Bellier, O., Sebrier, M., Beaudoiun, T., Villeneuve, M., Braucher, R., Bourles, D., Siame, L., Putranto, E., & Pratomo, I. (2001). High Slip Rate for a Low Seismicity Along the Palu-Koro Active Fault in Central Sulawesi (Indonesia). *Terra Nova, 13*, 463-470. Retrieved from https://www.geologie.ens.fr/~vigny/articles/tera-nova-382.pdf

Bellier, O., Sébrier, M., Seward, D., Beaudouin, T., Villeneuve, M., & Putranto, E. (2006). Fission Track and Fault Kinematics Analyses for New Insight into the Late Cenozoic Tectonic Regime Changes in West-Central Sulawesi (Indonesia). *Tectonophysics, 413*(3-4), 201–220. https://doi.org/10.1016/j.tecto.2005.10.036

Bradley, K., Mallick, R., Andikagumi, H., Hubbard, J., Meilianda, E., Switzer, A., Du, N., Brocard, G., Alfian, D., Benazir, B., Feng, G., Yun, S., Majewski, J., Wei, S., & Hill, E. M. (2019). Earthquake-Triggered 2018 Palu Valley Landslides Enabled by Wet Rice Cultivation. *Nature Geoscience, 12*, 935-939. https://doi.org/10.1038/s41561-019-0444-1

Charles, M. G. A., Ballantyne, P. D., & Hall, R. (1988). Mesozoic-Cenozoic rift-drift sequence of Asian fragments from Gondwanaland. *Tectonophysics, 155*(1-4), 317-330. https://doi.org/10.1016/0040-1951(88)90272-7

Chen, S. Y. S., Marchal, O., Lerner, P. E., McCorkle, D. C., & Rutgers van der Loeff, M. M. (2021). On the Cycling of ^{231}Pa and ^{230}Th in Benthic Nepheloid Layers. *Deep Sea Res, I*, 177, 103627, https://doi.org/10.1016/j.dsr.2021.103627

Cummins, P. R. (2019). Irrigation and the Palu Landslides. *Nature Geoscience, 12*, 881–882. https://doi.org/10.1038/s41561-019-0467-7

Grandis, H. (2009). *Pengantar Pemodelan Inversi Geofisika*. Jakarta: Himpunan Ahli Geofisika Indonesia.

Hazarika, H., Rohit, D., Pasha, S. M. K., Maeda, T., Mashyur, I., Arsyad, A., & Nurdin, S. (2021). Large Distance Flow-Slide at Jono Oge Due to the 2018 Sulawesi Earthquake, Indonesia. *Soils and Foundations, 60*(4), 239-255. https://doi.org/10.1016/j.sandf.2020.10.007

Helmers, H., Maaskant, P., & Hartel, T. H. D. (1990). Garnet Peridotite and Associated High-Grade Rocks from Sulawesi, Indonesia. *Lithos, 25*(1-3), 171-188. https://doi.org/10.1016/0024-4937(90)90013-Q

Hinze, W. J., Von Frese, R. R. B., & Saad, A. H. (2013). *Gravity and Magnetic Exploration Principles, Practices and Applications*. Cambridge: Cambridge University Press.

Jaya, A., Nishikawa, O., & Jumadil, S. (2019). Distribution and Morphology of the Surface Ruptures of the 2018 Donggala–Palu Earthquake, Central Sulawesi, Indonesia. *Earth Planets Space, 71*, 144. https://doi.org/10.1186/s40623-019-1126-3

Kiyota, T., Furuichi, H., Hidayat, R. F., Tada, N., & Nawir, H. (2020). Overview of Long-Distance Flow-Slide Caused by the 2018 Sulawesi Earthquake, Indonesia. *Soils and Foundations, 60*(3), 722-735. https://doi.org/10.1016/j.sandf.2020.03.015

Kramer, S. L. (1996). *Geotechnical Earthquake Engineering. Prentice-Hall civil engineering and Engineering Mechanics Serries*. Upper Saddle River 653: Prentice Hall.

Kusumawardani, R., Chang, M., Upomo, T. C., Huang, R. C., Fansuri, M. H., & Prayitno, G. A. (2021). Understanding of Petobo Liquefaction Flowslide by 2018.09.28 Palu-Donggala Indonesia Earthquake Based on Site Reconnaissance. *Landslides, 18*(9), 3163-3182. https://doi.org/10.1007/s10346-021-01700-x

Leeuwen, T., Allen, C. M., Elburg, M., Masonne, H., Palin, J. M., & Hennig, J. (2016). The Palu Metamorphic Complex, NM Sulawesi, Indonesia: Origin and Evaluation of a Young Metamorphic Terrane with Links to Gondwana and Sundaland.

Journal of Asian Earth Sciences, 155, 133-152. dx.doi.org/10.1016/j.jseaes.2015.09.025

Okamura, M., Ono, K., Arsyad, A., Minaka, U. S., & Nurdin, S. (2020). Large-Scale Flowslide in Sibalaya Caused by the 2018 Sulawesi Earthquake. *Soils and Foundations, 60*(4), 1050-1063. https://doi.org/10.1016/j.sandf.2020.03.016

Rahayu, W., Yuliyanti, I., & Bahsan, E. (2021). Analysis of potential liquefaction using cone penetration test data and grain size distribution test with case study of liquefaction in Lolu Village. In IOP Conference Series: Earth and Environmental Science (Vol. 622, No. 1, p. 012015). IOP Publishing. https://doi.org/10.1088/1755-1315/622/1/012015

Sawicki, A., & Mierczyński, J. (2009). On the Behaviour of Liquefied Soil. *Computers and Geotechnics, 36*(4), 531-536. https://doi.org/10.1016/j.compgeo.2008.11.002

Socquet, A., Hollingsworth, J., Pathier, E., & Bouchon, M. (2019). Evidence of Supershear During the 2018 Magnitude 7.5 Palu Earthquake from Space Geodesy. *Nat Geosci, 12*, 192–199. https://doi.org/10.1038/s41561-018-0296-0

Socquet, A., Simons, W., Vigny, C., McCaffrey, R., Subarya, C., Sarsito, D., Ambrosius, B., & Spakman, W. (2006). Microblock Rotations and Fault Coupling in SE Asia Triple Junction (Sulawesi, Indonesia) from GPS and Earthquake Slip Vector Data. *Journal of Geophysical Research Atmospheres, 111*, B08409. https://doi.org/10.1029/2005JB003963

Soekamto, R., & Sumadirdja, H. (1973). *Reconnaissance Geological Map of the Palu Quadrangle, Sulawesi, Skala 1 : 250.000*. Bandung: GRDC.

Sukarna, D., Sutisna, K., & Sukido, S. (1993). *Peta Geologi Lembar Pasangkayu, Sulawesi*. Bandung: Pusat Penelitian dan Pengembangan Geologi.

Telford, W. M., Geldart, L. P., & Sheriff, R. E. (1990). *Applied Geophysics* (2nd ed). Cambridge: Press Syndicate of the University of Cambridge. ISBN 0–521–32693-1.

Tsuchida, H. (1970). Prediction and Countermeasure Against Liquefaction in Sand Deposits. *Abstract of the Seminar of the Port and Harbour Research Institute*. Yokosuka, Japan: Ministry of Transport.

Watkinson, I. A., & Hall, R. (2019). Impact of Communal Irrigation on the 2018 Palu Earthquake-Triggered Landslides. *Nat Geosci, 12*, 940–945. https://doi.org/10.1038/s41561-019-0448-x

Watkinson, I. M., & Hall, R. (2017). Fault Systems of the Eastern Indonesian Triple Junction: Evaluation of Quaternary Activity and Implications for Seismic Hazards. *Geological Society, London, Special Publications, 441*, 71–120. https://doi.org/10.1144/sp441.8